Applied Physics Letters

Reducing interface recombination for $Cu(In,Ga)Se_2$ by atomic layer deposited buffer layers

Cite as: Appl. Phys. Lett. **107**, 033906 (2015); https://doi.org/10.1063/1.4927096
Submitted: 14 May 2015 . Accepted: 03 July 2015 . Published Online: 23 July 2015

Adam Hultqvist, Jian V. Li, Darius Kuciauskas, Patricia Dippo, Miguel A. Contreras, Dean H. Levi, and Stacey F. Bent

Reducing interface recombination for $Cu(In,Ga)Se_2$ by atomic layer deposited buffer layers

Adam Hultqvist,[1] Jian V. Li,[2] Darius Kuciauskas,[2] Patricia Dippo,[2] Miguel A. Contreras,[2] Dean H. Levi,[2] and Stacey F. Bent[1]
[1]*Department of Chemical Engineering, Stanford University, Stanford, California 94305, USA*
[2]*National Renewable Energy Laboratory, Golden, Colorado 80401, USA*

(Received 14 May 2015; accepted 3 July 2015; published online 23 July 2015)

Partial $CuInGaSe_2$ (CIGS) solar cell stacks with different atomic layer deposited buffer layers and pretreatments were analyzed by photoluminescence (PL) and capacitance voltage (CV) measurements to investigate the buffer layer/CIGS interface. Atomic layer deposited ZnS, ZnO, and SnO_x buffer layers were compared with chemical bath deposited CdS buffer layers. Band bending, charge density, and interface state density were extracted from the CV measurement using an analysis technique new to CIGS. The surface recombination velocity calculated from the density of interface traps for a ZnS/CIGS stack shows a remarkably low value of 810 cm/s, approaching the range of single crystalline II–VI systems. Both the PL spectra and its lifetime depend on the buffer layer; thus, these measurements are not only sensitive to the absorber but also to the absorber/buffer layer system. Pretreatment of the CIGS prior to the buffer layer deposition plays a significant role on the electrical properties for the same buffer layer/CIGS stack, further illuminating the importance of good interface formation. Finally, ZnS is found to be the best performing buffer layer in this study, especially if the CIGS surface is pretreated with potassium cyanide. © *2015 AIP Publishing LLC*. [http://dx.doi.org/10.1063/1.4927096]

$Cu(In,Ga)Se_2$ (CIGS) thin film solar cells constitute a promising technology that has recently reached a power conversion efficiency (η) of 21.7%.[1] Previously, the state-of-the-art CIGS solar cells used a CdS buffer layer within the solar cell stack due to its unparalleled performance. However, CdS has a band gap that is small enough to absorb the higher energy photons of the solar spectrum. Further improvements are therefore theoretically possible if CdS is replaced with a fully transparent layer, which motivated many studies of alternative buffer layers.[2] Recently, the effect of these studies has started to come to fruition with record performance for larger CIGS mini modules[3] and commercial production of full scale modules,[4] and it is therefore natural to continue these studies to further enhance the performance and understanding of these layers.

The best CdS alternatives found to date are In_2S_3 and the ZnO-based ternary compounds including Zn(O,S), (Zn,Mg)O, and ZnSnO.[3–8] Consistent with theory, the short circuit current density (J_{sc}) does increase due to the full transparency of the alternatives, but the cells typically lose open circuit voltage (V_{oc}), fill factor (FF), or both compared to CdS references, and thus, the overall η does not improve as much as theoretically predicted. The main reason for the losses is attributed to increased interface recombination at the buffer layer/CIGS interface as well as to reduced electron transport across the interface.[2,9,10]

In this study, we aim to shed further light on what governs the interface recombination between the alternative buffer layers and the CIGS absorber using the optical analysis methods of photoluminescence emission spectroscopy (PL) and time-resolved photoluminescence (TRPL), as well as the electrical analysis method capacitance-voltage (CV) measurements. We have chosen to make these measurements on a simplified solar cell stack where the binary compounds ZnO, ZnS, and SnO_x, which are subcomponents of some of the best alternative buffer layers, are deposited on CIGS/Mo/soda-lime glass (SLG) substrates and compared to a reference stack using a CdS buffer layer. While these partial stacks have a buffer/CIGS interface that operates under different conditions during CV measurements due to having a Hg contact with a different work function than the commonly used, heavily doped ZnO of a full stack,[11,12] we choose them because they make it easier to isolate the previously mentioned interface recombination of the buffer layer/CIGS interface during electrical measurements. Dissimilarities between the stacks due to diffusion of elements because of the increased thermal budget from the heavily doped ZnO deposition is not likely, based on previous studies.[8,13] The ZnO, ZnS, and SnO_x passivation materials have also been chosen because of their different conduction band offsets (CBO) towards CIGS[14–16] (see supplementary material, Fig. S1[17]). We also investigate the influence of different surface treatments prior to the buffer layer deposition. Furthermore, we identify a champion out of the materials and pretreatments that forms the most promising interface. In particular, we find that we can get a remarkably low surface recombination velocity (SRV) for certain stacks.

The CIGS/Mo/SLG stacks were fabricated at the National Renewable Energy Laboratory (NREL) using a state-of-the-art baseline process.[18,19] After the initial stack was completed at NREL, the samples were shipped to Stanford in an inert nitrogen atmosphere and stored in a nitrogen glove box until atomic layer deposition (ALD) of

the buffer layer. Prior to ALD, the CIGS surface was treated for 3 min with one of the following: 1 M ammonium hydroxide (NH_3), 1.5 M potassium cyanide (KCN), or 1.5 M hydrochloric acid (HCl). Following the treatment, the samples were rinsed in deionized (DI) water for 1 min. One sample of each batch was also kept untreated as a reference. ZnS and ZnO were deposited in a custom-built, convective-flow, hot-wall ALD reactor at 125 °C, described in detail in a previous study,[20] using a diethylzinc (DEZ) precursor and H_2S or H_2O as the counter reactant. Pulse lengths of the DEZ/N_2 purge/H_2S/N_2 purge steps used for the ZnS process were 1/30/0.25/30 s, respectively. For the ZnO process, the pulse lengths of the DEZ/N_2 purge/H_2O/N_2 purge steps were 1/30/1/30 s. SnO_x was deposited using a commercial hot-wall ALD reactor (Arradiance Gemstar 6) at 150 °C using tetra (dimethylamino)tin (TDMA Sn) as the Sn precursor and H_2O as the counter reactant. For the SnO_x process, TDMA Sn/N_2/H_2O/N_2 pulse lengths were 1/60/0.5/60 s, respectively. To create references for the ALD films, CdS was deposited using chemical bath deposition (CBD) on CIGS samples. CdS CBD was carried out at Stanford for 13 min at 60 °C in a jacketed beaker using 36.6 ml of 14.8 M ammonium hydroxide, 2.5 ml of 1.5 M thiourea, and 5 ml of 0.015 M cadmium sulfate.

A spectroscopic ellipsometer (J. A. Woolam Co., Inc. α-SE) was used to model the buffer layer thicknesses. Three different measurements at incidence angles of 65°, 70°, and 75° with a wavelength range of 380–890 nm were used for the thickness modeling. The PL measurements were taken at room temperature using a 632.8 nm HeNe laser at a power of 5 mW. Peak fitting with IGOR Pro software was used to model the total intensity of the PL peaks for each sample. A Yb:KGW laser and an optical parametric amplifier (Pharos/Orpheus, Light Conversion) with 0.3 ps pulses and 1.1 MHz repetition rate were used for TRPL measurements. The excitation wavelength was 650 nm, the average power was 0.35 mW, and the excitation beam diameter was 0.2 mm. A photomultiplier (Hamamatsu R5509) and single photon counting electronics (Picoharp 300, Picoquant) were used for time-correlated single photon counting. Spectrally integrated photoluminescence was measured with 1050 nm long pass filter. Spectrally integrated TRPL dynamics could be described as single exponential with lifetime τ_{TRPL};[21] this model was used in our data analysis. The CV measurements were carried out using an Agilent 4294 A impedance analyzer on a metal-insulator-semiconductor (MIS) structure consisting of an Hg probe, the buffer layer, and the CIGS absorber with Mo as the back-contact. The room-temperature CV data measured at 100 kHz with an AC voltage of 35 mV exhibited typical high-frequency characteristics with the lack of a strong accumulation regime evident from the not-so-flat upper plateau. We calibrated the actual area of the Hg contact by matching the bulk doping of the CIGS absorber extracted from the depletion regime of the MIS structure to that measured from completed front-contact-metal/Al-doped-ZnO/CdS/CIGS/Mo-back-contact p-n junction devices ($N_A = 6.0 \times 10^{15}\,cm^{-3}$). While this approach does not consider bulk doping differences between the stacks due to different band bending, it gives a reference point for the partial stack that is likely not too dissimilar from the full stack and it enables us to compare the partial stacks to each other. We also used the thicknesses of the buffer layers measured by ellipsometry as an input parameter rather than extracting them from the weak accumulation regime as it is a more accurate approach. The density of trapped charges per volume in the insulator (Q_t), or in this study the buffer layer, is a measure of how many charges are present in the insulator away from the interface. Determining Q_t is an established way for silicon MIS structures to separate effects seen in CV from the SiO_x/Si interface and the SiO_x bulk.[22] Q_t and the band bending (BB) were extracted using the standard high-frequency CV method on metal-insulator-semiconductor (MIS) structures.[22]

As shown in Fig. 1, there are significant differences in the PL emission characteristics when the different buffer layers are used. First, we observe changes in the PL spectra. PL emission spectra for CIGS are typically analyzed using Gaussian line shapes.[23–26] In this study, we choose to use three Gaussians for the fitting because the tails on the lower energy side are not Gaussian for ZnO and SnO_x; this feature can sometimes be seen as an extra peak, yielding three prominent peaks on this type of CIGS and has previously been reported by Sakurai *et al.*[23] Attempts to correlate the Gaussian sub-bands to bulk and grain boundaries were inconclusive,[25,27,28] and Gaussian components are assumed to indicate emission due to defects and defect bands. Our data (Fig. 1) show that all three Gaussian sub-bands are influenced by the buffer layer, and they can therefore not be attributed solely to the absorber, but must also have contributions from interface effects. The low energy peak has the lowest amplitude, whereas the middle and high energy peaks change in their relative intensity distribution as illustrated in Fig. 1.

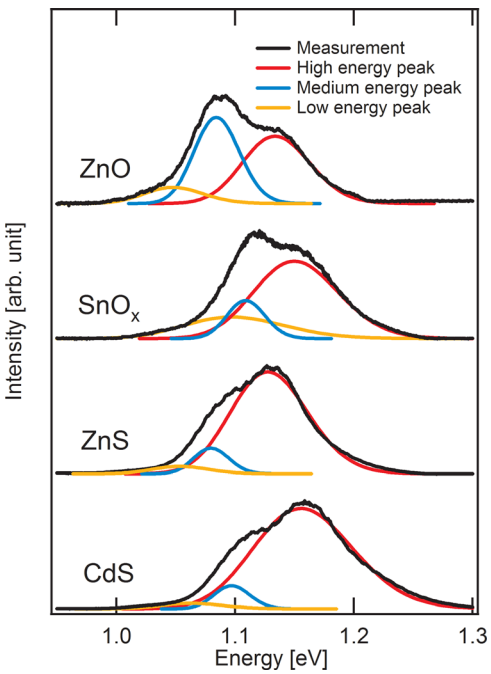

FIG. 1. Normalized PL emission spectra for CIGS with ZnS, ZnO, SnO_x, and CdS ALD buffers. Experimental data are shown in black. The Gaussian fits to the low, intermediate, and high energy peaks are displayed in yellow, blue, and red, respectively.

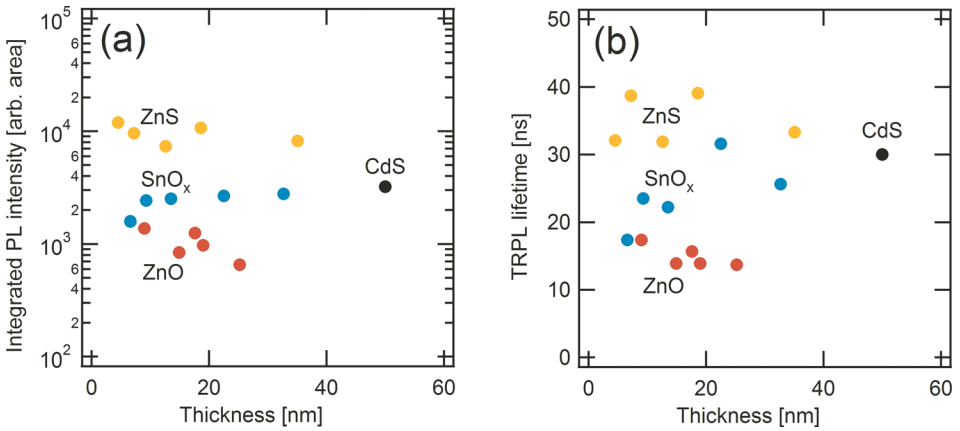

FIG. 2. (a) Total integrated PL intensity vs thickness and (b) TRPL lifetime, τ_{TRPL} vs thickness for CIGS absorbers with several ALD buffer layers: ZnS (yellow), ZnO (red), SnO_x (blue), and CdS (black).

Next, we analyze integrated PL emission intensity (Fig. 2(a)) as a function of buffer layer type and thickness. The integrated intensity increases by about an order of magnitude overall when changing buffers from ZnO → SnO_x → CdS → ZnS. The strongest PL emission is observed for the ZnS buffer, which is consistent with a large CBO hindering electron drift and/or diffusion into the buffer layer from the CIGS. This effectively increases the concentration of excited electrons that radiatively recombine within the CIGS. The much weaker PL emission observed for the ZnO buffer could indicate electron drift from CIGS to ZnO due to a lower CBO for ZnO and/or an increased amount of surface charge. According to the estimated band diagram shown in Fig. S1, the CBO for the SnO_x buffer is similar to that for ZnO, but the PL emission intensity for SnO_x is approximately three times stronger than that for ZnO (see supplementary material).[17]

The TRPL data (Table I and Fig. 2(b)) are consistent with the trends observed in the integrated PL emission intensity. We find that τ_{TRPL} does not depend on the buffer layer thickness but is sensitive to the buffer layer type, where τ_{TRPL} for the NH_3-treated samples was 30 ± 2 ns for CdS, 35 ± 4 ns for ZnS, 25 ± 6 ns for SnO_x, and 15 ± 2 ns for ZnO. The independence on buffer layer thickness suggests that τ_{TRPL} primarily depends on bulk CIGS or buffer/CIGS interface properties, but not on bulk properties of the buffer layer. The result thus indicates that ALD buffers change either the interface or the CIGS absorber properties to at least several hundred nm (the light absorption depth in this material).

TABLE I. Comparison of the integrated PL emission intensity and lifetime τ_{TRPL} for different passivation layers and pretreatments.

Buffer	Thickness (nm)	Treatment	$PL_{total\ int.}$ (normalized)	τ_{TRPL} (ns)
SnO_x	23	NH_3	0.84	32
	24	KCN	1.7	38
	24	HCl	0.56	23
	23	Untreated	1.7	36
ZnS	19	NH_3	3.4	39
	18	KCN	4.4	46
	18	HCl	1.3	25
	20	Untreated	3.8	43
ZnO	19	NH_3	0.30	14
	22	KCN	0.56	20
	20	HCl	0.34	16
	14	Untreated	1.7	26
CdS	50	Untreated	1	30

We also investigate the correlation between absorber pretreatments and PL intensity/τ_{TRPL}. Data in Table I show that both intensity and τ_{TRPL} increase as the pretreatment changes from HCl → NH_3 → untreated → KCN with the exception of ZnO (where the KCN treatment and the untreated sample change order). This result is in agreement with previous studies where KCN has been shown to clean CIGS surfaces of oxides and other contaminants that introduce recombination sites that can affect the PL signal and its lifetime.[29–31] Both the NH_3 and HCl treatments are detrimental in that they reduce both the PL intensity and the τ_{TRPL} when compared to the untreated samples. Although the nature of this effect requires further study, we note that the reagents can affect the chemical environment of the surface (potentially selectively etching Cu out of the CIGS film), which in turn could change the nucleation of the subsequent ALD growth enough to modify the buffer layer/CIGS interface.

CV measurements were carried out on MIS stacks made with each buffer layer. The stacks with ZnO and SnO_x were found to have non-ideal MIS diode characteristics, most likely due to these ALD layers being too conductive. Results on ZnO and SnOx are not included in further discussion and we focus instead on ZnS.

Fig. 3(a) shows that Q_t is negative and decreases in magnitude as the thickness of the ZnS layer increases. Q_t also depends on pretreatment. There is no straightforward explanation for this observation based on our data, but we speculate that charges may be trapped at the interface in the form of native oxides and carbonates formed during the air exposure of the samples prior to ALD deposition.[31,32] Depending on the pretreatment, different amounts of these oxides and carbonates may be removed from the surface, and thus, Q_t might vary because of this. The Q_t trend could in this manner be the result of a large negative charge trapped at the interface with a subsequent film growth of a slightly positive film, lowering the overall negative charge as it grows thicker. For the CdS sample the charge is found to be positive. In addition, the extracted BB increases for thicker ZnS layers, Fig. 3(b). This behavior indicates that the quasi Fermi level splitting between the buffer layer and the CIGS materials has increased, which could either be an increase of positive charges in the buffer layer or at the interface, or an increase of negative charges in the CIGS itself as the buffer layer grows thicker.[22] We suggest that it is due to an increase of

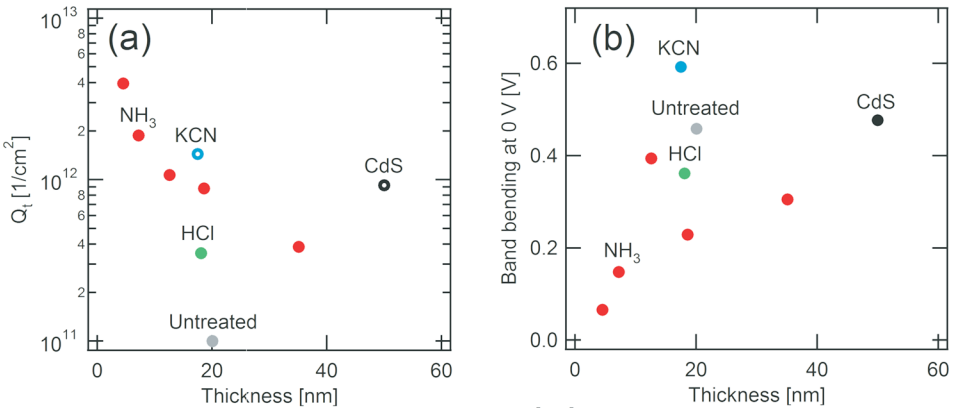

FIG. 3. (a) Magnitude of Q_t vs thickness for ZnS as a function of the film thickness and CIGS pretreatment, where red represents NH_3, green HCl, cyan KCN, gray untreated, and black CdS, and where open markers represent positive charges and filled markers represent negative charges. (b) Band bending vs thickness for ZnS and CdS.

positive charges in the buffer layer due to the trends in Q_t; see Fig. S2 in the supplementary material for a more detailed explanation.[17] Although Q_t and BB each varied with ZnS thickness, the PL emission intensity was independent of thickness, reaffirming that the differences seen in PL emission are mainly due to CIGS bulk changes or the buffer/CIGS interface. It is however possible that that the effects of BB are much weaker than the CIGS bulk effects. In the case of BB, the effect of the increased electric field due to an increased BB drifting the electrons away and lowering the PL emission[33] could be inhibited by the spike in the conduction band for stacks with ZnS.[15]

To compare the trends between the optical and electrical measurements, we followed previously developed methods for estimating the V_{oc} from τ_{TRPL}[34] and from BB.[35] The τ_{TRPL} approach estimates a V_{oc} of 686 mV for the NH_3 pretreated ZnS sample and 696 mV for the KCN pretreated one, with the CdS reference yielding a comparable value of 698 mV. Several complete PV devices were fabricated at NREL from the CIGS substrate used in our study, and an average $V_{oc} = 694$ mV was found under AM1.5 illumination. The good agreement suggests that our PL lifetime analysis for the partial device gives accurate estimates for the final performance. Similarly, V_{oc} for the ZnS samples was estimated from BB to be 334 mV for a NH_3 treated sample, 502 mV for a KCN treated sample, and 403 mV for the CdS reference sample. These values are all substantially lower than the reference value from the full devices, showing that estimating the V_{oc} of the full stack through BB is not as straightforward, especially since the effects of the heavily doped transparent conducting oxide is omitted in the analysis. Nevertheless, the trends from both estimation approaches agree well, showing that there may be a correlation between a long τ_{TRPL} and a large BB. Using the formulation provided in a previous study[36] and experimentally extracted parameters,[37] we can estimate the SRV from the calculated D_{it}, described and shown (Fig. S3) in detail in the supplementary material.[17] We find it to be 810 cm/s for the best NH_3-treated ZnS sample, 8400 cm/s for the KCN-treated sample, and 14 000 cm/s for the CdS reference. 810 cm/s is a low value compared to previous studies on polycrystalline solar cell materials and is approaching results achieved for single crystalline systems. For example, the lowest recombination velocity for a double heterostructure fabricated with epitaxial MgCdTe/CdTe/MgCdTe is S = 470 cm/s.[38] It is surprising that the SRV is so high for the KCN ZnS and CdS samples, which otherwise perform well in this study. However, it is possible that the influence of the SRV on the other measurements is limited. Previous studies suggests that there is a large positive CBO at the ZnS/CIGS interface[15] and that such an offset would type invert the top of the CIGS bulk, which in turn reduces the influence of the SRV on the overall recombination of the solar cell.[10]

In conclusion, we have evaluated ZnO, SnO_x, and ZnS as passivation and buffer layers for CIGS/Mo/SLG stacks and compared them to reference stacks using CdS. The buffer layer choice is found to affect the PL spectrum and the TRPL lifetimes in a way that suggests the buffer layer affects the buffer/CIGS or the CIGS bulk itself either chemically or through changes in the built in electric field. ZnS is found to have the best passivation performance out of all the CdS alternatives studied here for several reasons. It has the strongest PL response and the longest TRPL lifetimes, even better than CdS. Furthermore, ZnS is found to have excellent electrical properties such as a low D_{it} and a strong BB compared to CdS. Depending on the technique used in the analysis, an estimated theoretical increase of 0–100 mV in V_{oc} over CdS is found for KCN-treated samples with ZnS. We also find that one of the samples with a ZnS buffer has a remarkably low SRV of 810 cm/s, which is approaching that of epitaxially grown MgCdTe/CdTe/MgCdTe double heterostructures. The PL and electrical measurements also show that pretreatments have a big effect on the resulting interface. Especially, diluted KCN gives superior performance compared to diluted ammonium hydroxide and diluted HCl, both of which are found to lead to poorer performance than even the untreated samples.

This study was conducted under the Center on Nanostructuring for Efficient Energy Conversion at Stanford University (A.H. and S.F.B.). The Marcus and Amalia Wallenberg Foundation are acknowledged for supporting through the Stig Hagström Stipend (A.H.). Finally, this work was supported by the National Renewable Energy Laboratory as a part of the Non-Proprietary Partnering Program under Contract No. De-AC36-08-GO28308 with the U.S. Department of Energy (J.V.L., D.K., P.D., M.A.C., and D.H.L.).

[1]P. Jackson, D. Hariskos, R. Wuerz, O. Kiowski, A. Bauer, T. M. Friedlmeier, and M. Powalla, Phys. Status Solidi RRL **9**, 28 (2015).
[2]N. Naghavi, D. Abou-Ras, N. Allsop, N. Barreau, S. Bücheler, A. Ennaoui, C.-H. Fischer, C. Guillen, D. Hariskos, J. Herrero, R. Klenk, K. Kushiya, D.

Lincot, R. Menner, T. Nakada, C. Platzer-Björkman, S. Spiering, A. N. Tiwari, and T. Törndahl, Prog. Photovoltaics **18**, 411 (2010).
[3]H. Sugimoto, in *40th IEEE Photovoltaic Specialist Conference, Denver, CO* (IEEE, 2014), pp. 2767–2770.
[4]K. Kushiya, Sol. Energy Mater. Sol. Cells **122**, 309 (2014).
[5]M. Nakamura and Y. Kouji, in *39th IEEE Photovoltaic Specialist Conference, Tampa, FL* (IEEE, 2013), pp. 0849–0852.
[6]N. Naghavi, S. Spiering, M. Powalla, B. Cavana, and D. Lincot, Prog. Photovoltaics **11**, 437 (2003).
[7]A. Hultqvist, C. Platzer-Björkman, T. Törndahl, M. Ruth, and M. Edoff, in *Proceedings of the 22nd European Photovoltaics Solar Energy Conference, Milan* (WIP – Renewable Energies, 2007), pp. 2381–2384.
[8]J. Lindahl, J. T. Wätjen, A. Hultqvist, T. Ericson, M. Edoff, and T. Törndahl, Prog. Photovoltaics **21**, 1588 (2013).
[9]S. Siebentritt, Sol. Energy Mater. Sol. Cells **95**, 1471 (2011).
[10]A. Niemegeers, M. Burgelman, and A. De Vos, Appl. Phys. Lett. **67**, 843 (1995).
[11]H. B. Michaelson, J. Appl. Phys. **48**, 4729 (1977).
[12]X. Jiang, F. L. Wong, M. K. Fung, and S. T. Lee, Appl. Phys. Lett. **83**, 1875 (2003).
[13]T. Törndahl, E. Coronel, A. Hultqvist, C. Platzer-Björkman, K. Leifer, and M. Edoff, Prog. Photovoltaics **17**, 115 (2009).
[14]M. Kapilashrami, C. X. Kronawitter, T. Törndahl, J. Lindahl, A. Hultqvist, W.-C. Wang, C.-L. Chang, S. S. Mao, and J. Guo, Phys. Chem. Chem. Phys. **14**, 10154 (2012).
[15]C. Platzer-Björkman, T. Törndahl, D. Abou-Ras, J. Malmström, J. Kessler, and L. Stolt, J. Appl. Phys. **100**, 044506 (2006).
[16]T. Schulmeyer, R. Hunger, A. Klein, W. Jaegermann, and S. Niki, Appl. Phys. Lett. **84**, 3067 (2004).
[17]See supplementary material at http://dx.doi.org/10.1063/1.4927096 for detailed information regarding band alignment, calculated density of interface traps, and the proposed relation between the trapped oxide charge and the band bending.
[18]K. Ramanathan, M. A. Contreras, C. L. Perkins, S. Asher, F. S. Hasoon, J. Keane, D. Young, M. Romero, W. Metzger, R. Noufi, J. Ward, and A. Duda, Prog. Photovoltaics **11**, 225 (2003).
[19]I. Repins, M. A. Contreras, B. Egaas, C. DeHart, J. Scharf, C. L. Perkins, B. To, and R. Noufi, Prog. Photovoltaics **16**, 235 (2008).
[20]M. N. Mullings, C. Hägglund, and S. F. Bent, J. Vac. Sci. Technol., A **31**, 061503 (2013).
[21]W. K. Metzger, I. L. Repins, and M. A. Contreras, Appl. Phys. Lett. **93**, 022110 (2008).
[22]*Physics of Semiconductor Devices*, 3rd ed. edited by S. M. Sze and K. K. Ng (Wiley, 2006).
[23]T. Sakurai, K. Taguchi, M. M. Islam, S. Ishizuka, A. Yamada, K. Matsubara, S. Niki, and K. Akimoto, Jpn. J. Appl. Phys. **50**, 05FC01 (2011).
[24]R. Bacewicz, P. Zuk, and R. Trykozko, Opto-Eelectron. Rev. **11**, 277 (2003).
[25]L. Gütay and G. Bauer, Thin Solid Films **515**, 6212 (2007).
[26]L. Van Puyvelde, J. Lauwaert, S. Nishiwaki, P. F. Smet, D. Poelman, A. N. Tiwari, and H. Vrielinck, J. Phys. D. Appl. Phys. **47**, 045102 (2014).
[27]M. J. Romero, H. Du, G. Teeter, Y. Yan, and M. M. Al-Jassim, Phys. Rev. B **84**, 165324 (2011).
[28]L. Gütay, C. Lienau, and G. H. Bauer, Appl. Phys. Lett. **97**, 052110 (2010).
[29]Y. Hashimoto, N. Kohara, T. Negami, M. Nishitani, and T. Wada, Jpn. J. Appl. Phys. **35**, 4760 (1996).
[30]L. Weinhardt, O. Fuchs, D. Groß, E. Umbach, C. Heske, N. G. Dhere, A. A. Kadam, and S. S. Kulkarni, J. Appl. Phys. **100**, 024907 (2006).
[31]S. Merdes, A. Steigert, F. Ziem, I. Lauermann, R. Klenk, F. Hergert, C. A. Kaufmann, and R. Schlatmann, Thin Solid Films **574**, 28 (2015).
[32]G. Dingemans, N. M. Terlinden, M. A. Verheijen, M. C. M. van de Sanden, and W. M. M. Kessels, J. Appl. Phys. **110**, 093715 (2011).
[33]M. Igalson, M. Pawłowski, and D. Prządo, Opto-Electron. Rev. **19**, 435 (2011).
[34]I. L. Repins, W. K. Metzger, C. L. Perkins, J. V. Li, and M. A. Contreras, IEEE Trans. Electron Devices **57**, 2957 (2010).
[35]A. Yamada, K. Matsubara, K. Sakurai, S. Ishizuka, H. T. Hajime, S. T. Baba, Y. Kimura, S. Nakamura, H. Nakanishi, and S. Niki, *Symposium F – Thin-Film Compound Semiconductor Photovoltaics Series: MRS Proceedings*, Vol. 865 (MRS Proceedings, 2005), p. F5.19.
[36]W. D. Eades and R. M. Swanson, J. Appl. Phys. **58**, 4267 (1985).
[37]J. V. Li, L. M. Mansfield, B. Egaas, and K. Ramanathan, in *45th IEEE Semiconductor Interface Specialists Conference San Diego* (IEEE, 2014), p. 11.11.
[38]X. Zhao, M. DiNezza, and S. Liu, Appl. Phys. Lett. **105**, 252101 (2014).